Anion Photoelectron Spectroscopy and Density Functional Investigation of Diniobium−Carbon Clusters

K. L. Knappenberger, Jr.,[†,#] P. A. Clayborne,[§] J. U. Reveles,[§] M. A. Sobhy,[†] C. E. Jones, Jr.,[†] U. U. Gupta,[†] S. N. Khanna,[§] I. Iordanov,[‡] J. Sofo,[‡] and A. W. Castleman, Jr.[†,‡,*]

Departments of [†]Chemistry and [‡]Physics, The Pennsylvania State University, University Park, Pennsylvania 16802, and [§]Department of Physics, Virginia Commonwealth University, Richmond, Virginia 23284-2000. [#]Current address: University of California, Berkeley, and Lawrence Berkeley National Laboratory.

ABSTRACT Experimental photoelectron and computational results show diniobium−carbon (Nb_2C_n) clusters to coexist in multiple structural isomers: three-dimensional geometries, planar rings, and linear chains. Three-dimensional clusters having up to five carbons are formed preferentially with Nb−Nb bonding, whereas only Nb−C bonding is observed experimentally at six carbons. Clusters consisting of an odd number of atoms are also observed with linear geometries. The larger binary clusters ($n \geq 7$) display properties similar to those of pure carbon clusters. We provide evidence for niobium substitution of carbon atoms.

KEYWORDS: cluster-assembled materials · transition-metal clusters · anion photoelectron spectroscopy · cluster structure · carbon clusters

Clusters often portray strikingly different chemical and physical properties than their bulk counterparts, and, perhaps more intriguingly, these properties vary widely with cluster size and composition. Clusters are of interest as potential building blocks of new materials and as model catalysts, and, in terms of metal–carbon clusters, they provide insights into the formation, stability, and electronic characteristics of metal–carbon junctions. One example observed in metal–carbon clusters is the class known as metallocarbohedrenes (Met-Cars), which was discovered in our laboratory.[1] Met-Cars, of stoichiometry M_8C_{12}, where M is an early transition metal, are cage-like clusters that display enhanced stability in the gas phase and exhibit low ionization energies,[2] delayed ionization,[3] and unique relaxation dynamics.[4] Collectively, these findings imply that Met-Cars possess some amount of free electron character. Recently, it has been suggested that these clusters may be effective hydrodesulfurization catalysts.[5] Implementing cluster-assembled materials (CAMs), however, requires their production on larger scales and especially a more thorough understanding of the electronic properties of matter at finite dimensions. Currently, research in our group and others[6,7] is directed toward elucidating the interplay between transition metals and carbon, with an emphasis on understanding how the properties of their complexes evolve with size.

Of the many metal–carbon complexes, niobium carbides exhibit rather interesting properties. Previous research from our group[8,9] indicates that variations in cluster source conditions result in two dominant cluster structure types: Met-Cars and nanocrystallite species, with the niobium system being the most facile in displaying the transition between structures. The early study also demonstrated kinetic control over the cluster type formed. Ion mobility experiments conducted by Jarrold and coworkers[10] revealed that fullerenes readily incorporate niobium atoms by carbon replacement, an early finding suggesting that niobium can substitute carbon atoms. Currently, there is little understanding of this phenomenon; nonetheless, the many structural motifs of niobium−carbon clusters may present a very versatile system to direct the assembly of future CAMs. As reported herein, we have taken a systematic approach to addressing this problem by analyzing the electronic and geometric structures of diniobium−carbon clusters through a combination of photoelectron spectroscopy and density functional theory (DFT) studies. The results clearly show that multiple isomers are formed during the nucleation process. Of these, direct evidence for formation of linear $Nb_2C_n^-$ chains is obtained for binary clusters that include an odd number of carbon atoms. The nature of the niobium−carbon interaction is also found to change with cluster size. The Nb_2C_4 and Nb_2C_5 clusters contain niobium−niobium bonding, but in going

*Address correspondence to awc@psu.edu.

Received for review August 14, 2007 and accepted October 23, 2007.

Published online November 10, 2007.
10.1021/nn700167c CCC: $37.00

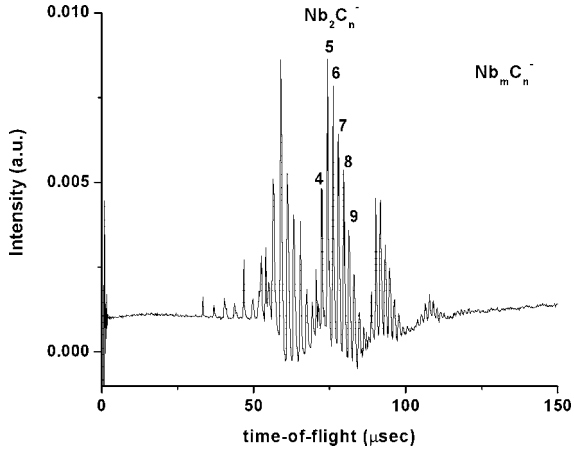

Figure 1. Anionic mass distribution of $Nb_mC_n^-$ clusters formed under high (>10%) methane/helium. The $Nb_2C_n^-$ series, studied here, is labeled.

to Nb_2C_6, niobium−carbon interactions become dominant.

The instrument and experimental procedure have previously been described in detail.[11] A typical anionic niobium−carbon cluster distribution is shown in Figure 1. Diniobium−carbon clusters are generated in a 10 Hz laser vaporization plasma reactor source. The second harmonic (532 nm, 1 mJ/pulse) of a Nd:YAG laser is focused on a translating and rotating rod, forming a plasma. A helium carrier gas seeded with 10% methane is passed over the plasma, leading to the formation of metal–carbon clusters. Clusters are formed over a range of sizes, but only the diniobium series, of interest here, is labeled. Photoelectron spectra of Nb_2C_n (n = 4–9) clusters, taken with our laser-based magnetic bottle time-of-flight apparatus at 4.0 eV detachment energy, are shown in Figure 2. The energy associated with each peak was ascertained by fitting each spectral feature to a Gaussian function and reporting the center energy as the electron binding energy. All measured electron binding energies are reported in Table 1, along with standard deviations determined to 2σ. The vertical detachment energy of $Nb_2C_4^-$ is determined to be 1.67 ± 0.13 eV, which corresponds to the lowest binding energy feature, and a second peak is measured at 2.25 ± 0.13 eV. As evidenced by the spectra in Figure 2 and the values reported in Table 1, an increase in cluster size is accompanied by a corresponding small but gradual shift to higher binding energies. A third, less intense feature in the $Nb_2C_4^-$ photoelectron spectra at 3.19 ± 0.13 eV is also present. A high-binding-energy feature is observed for all cluster sizes up to and including diniobium clusters bound to nine carbon atoms, which shifts to lower binding energy upon going from the $Nb_2C_4^-$ to the $Nb_2C_5^-$ species. Cluster sizes n = 4–6 display photoelectron spectra with the peak at lower binding energy appearing as the most intense feature. A transition is observed at n = 7, and the high-binding-energy feature becomes the most intense. At n = 8, only a

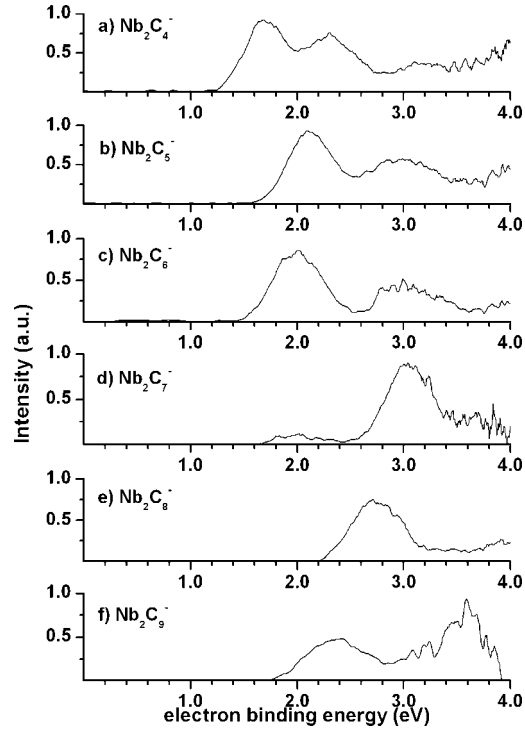

Figure 2. Anion photodetachment spectra of $Nb_2C_n^-$ clusters (n = 4–9). Measured photoelectron counts are reported as a function of electron binding energy (eV). All spectra are obtained with fixed photodetachment energy (4.0 eV).

single feature corresponding to a binding energy of 2.75 ± 0.14 eV is observed, whereas the spectrum of the n = 9 cluster contains a feature at 2.37 ± 0.13 eV as well as one at 3.57 ± 0.09 eV binding energy. All electron binding energy assignments are reported in Table 1.

To aid in the assignment of the experimentally measured electron spectra, we have carried out a first-principle electronic structure investigation on Nb_2C_n clusters in a generalized gradient approximation (GGA) within the density functional formalism.[12] Full geometry optimizations were performed using the deMon2k software.[13] In order to avoid the calculation of four-center electron repulsion integrals, the variational fitting of the Coulomb potential[14,15] was employed. The numerical integration of the exchange-correlation energy and potential was performed on an adaptive grid.[16] The exchange and correlation effects were incor-

TABLE 1. Measured Electron Binding Energies (eV)[a]

cluster	low energy	high energy
$Nb_2C_4^-$	X 1.67 ± 0.13	X 3.19 ± 0.13
	A 2.25 ± 0.13	
$Nb_2C_5^-$	X 2.13 ± 0.11	X 2.91 ± 0.14
$Nb_2C_6^-$	X 2.00 ± 0.16	X 3.02 ± 0.13
$Nb_2C_7^-$	X 2.01 ± 0.14	X 3.06 ± 0.15
$Nb_2C_8^-$	X 2.75 ± 0.14	
$Nb_2C_9^-$	X 2.37 ± 0.13	X 3.57 ± 0.09

[a]Experimentally measured electron binding energies determined from Gaussian fit. Standard deviation determined to within 2σ.

porated using the functional proposed by Perdew, Burke, and Ernzerhof.[17] In this study, we used the double-ζ valence polarized (DZVP) basis set[18] for the carbon atoms, and the Nb atom was described using the 13-electron scalar quasi-relativistic effective core potential (QECP) proposed by Andrae *et al.*[19] in combination with the LANL2DZ[20] valence basis. The auxiliary density was expanded in primitive Hermite Gaussian functions using the A2 auxiliary function set for C atoms and the GEN-A2* auxiliary function set for Nb. A half-numeric integrator was employed for the effective core potential (ECP) integrals.[21]

Several different bonding arrangements, including three-dimensional nonplanar cages, linear chains, and bicyclic rings, were considered. The stable isomeric structures relevant to these studies are shown in Figure 3. The findings are in relative agreement with those of Harris and Dance,[22] where the geometry of the Nb_2C_2 cluster was determined. The results of the calculations suggest that the ground-state structure of the 2,2 species is that of a planar rectangle with alternating Nb−C bonds. The most stable structure found has Nb−C distances of 1.94 Å and Nb−Nb distances of 2.72 Å and a nonbonding HOMO for the neutral. Investigation of other isomers revealed that the formation of Nb−C bonds is stabilizing, whereas Nb−Nb dissociation occurs without a barrier. It is evident, then, that the Nb_2C_2 cyclic ring forms in a way that maximizes the number of niobium−carbon interactions, followed by C−C interactions, both of which are preferential to Nb−Nb bonds. For all sizes considered here, the calculated lowest energy structure corresponded to a three-dimensional geometry. The computational results indicate that planar rings are stable for cluster sizes up to and including $Nb_2C_6^-$, but not for the larger clusters. However, a linear structure converges for all cluster sizes.

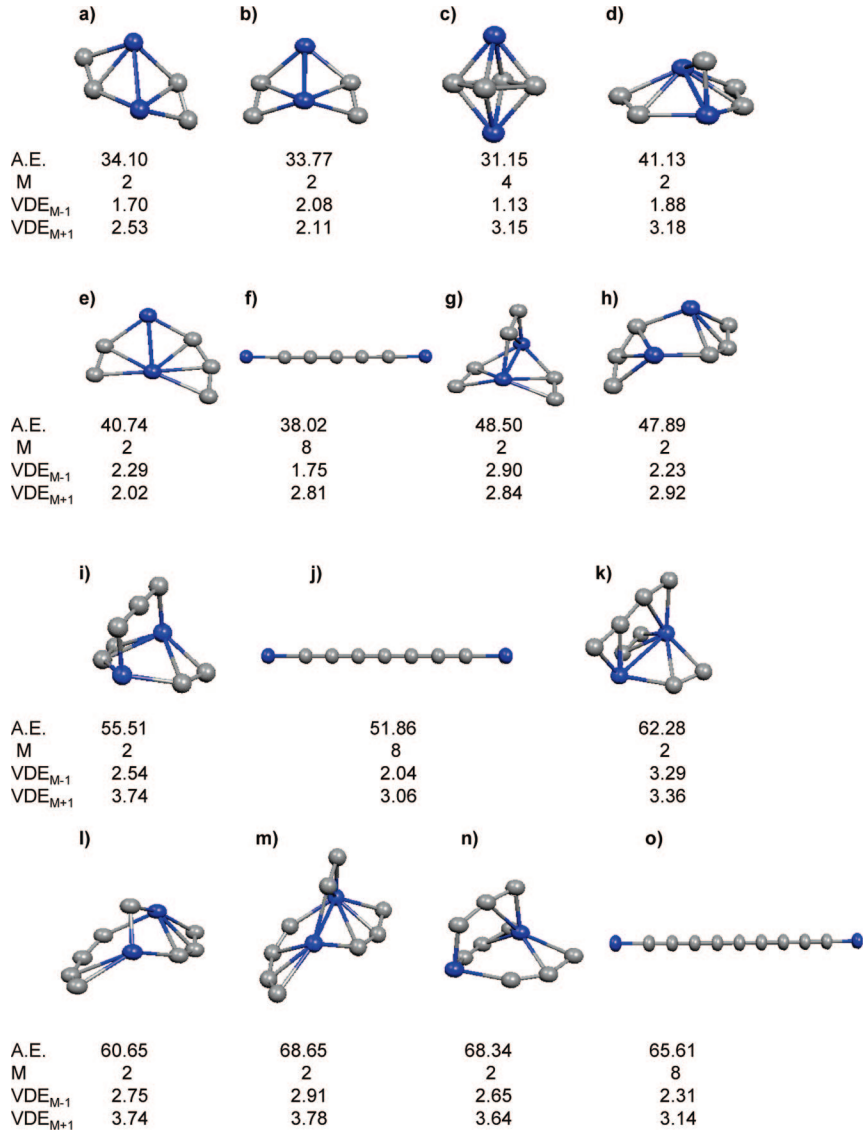

Figure 3. Optimized structures and computed atomization energy (AE), multiplicity (M), and vertical detachment energies (VDE) of M + 1 and M − 1 states (VDE_{M+1} and VDE_{M-1}, respectively). AE and VDE are given in electronvolts. Geometric structures are presented as follows: $Nb_2C_4^-$ (a−c), $Nb_2C_5^-$ (d−f), $Nb_2C_6^-$ (g,h), $Nb_2C_7^-$ (i,j), $Nb_2C_8^-$ (k,l), and $Nb_2C_9^-$ (m−o). Blue corresponds to niobium atoms, while gray represents carbon atoms.

Figure 3 shows the results of theoretical investigations. For each cluster we have listed the atomization energy (AE), indicating the energy required to break the cluster into individual atoms/ion. In order to make a comparison with negative-ion photodetachment spectra, we also calculated the vertical detachment energy (VDE) that represents the energy required to make a vertical transition from an anion with multiplicity M to the neutral species (of the same geometry) with multiplicity M + 1 and M − 1. The calculated VDEs are also reported below each geometric structure.

Comparing the three experimentally measured photoelectron peaks for $Nb_2C_4^-$ to the theoretical works, the coexistence of multiple isomers is clear. The peak corresponding to an electron binding energy of 1.67 eV is in good agreement with computational predictions for photodetachment from the doublet anion to neutral state for the isomer shown in Figure 3a, the minimum energy structure. The structure is three-dimensional and consists of two NbC_2 units, with Nb−Nb bonding at the center. Structurally, this isomer is similar to V_2C_4, which we published previously.[23] The

feature appearing with 2.25 eV could arise from photodetachment to the triplet state of the minimum energy isomer (Figure 3a), or it could correspond to the triplet-state transition of the structure shown in Figure 3b. The computational predictions for both are within the experimental uncertainty. Support for the assignment of the 2.25 eV transition to the triplet state of the isomer in Figure 3b is gained when looking at the growth pattern of larger clusters, as discussed below. Geometrically, the difference between the two isomers is an out-of-plane distortion for minimum energy, but both are very similar and contain Nb−Nb bonding. The less intense, higher binding energy feature at 3.19 eV matches well with predictions for the transition from the quartet to the quintet state of the structure seen in Figure 3c. The computationally predicted VDE for this structure is 3.15 eV. The corresponding 1.15 eV transition, corresponding to the triplet-state transition, is not observed. This peak likely overlaps with the intense peak measured at 1.67 eV, corresponding to the singlet-state transition of the minimum energy structure. The calculated atomization energy of the structure in Figure 3c is approximately 3 eV less than that of the minimum energy structure (Figure 3a). This finding is suggestive of high cluster source temperatures, likely owing to the carbon-rich expansion. Also, the contribution of neutral excited electronic states to experimentally measured higher binding energy features cannot be ruled out.

When going to $Nb_2C_5^-$, the lowest measured binding energy is 2.13 ± 0.11 eV, in relative agreement with the theoretically predicted value of 2.02 eV for the vertical detachment from the doublet state of the anion to the triplet state of the isomer shown in Figure 3e, which corresponds to the planar two-dimensional structure. Likewise, the experimentally measured peak at higher binding energy, 2.91 eV, matches the computational result for the transition from a spin multiplicity of 8 to the higher state of the linear isomer (Figure 3f). It should be noted that, within experimental uncertainty, the measured electron kinetic energy overlaps with that predicted for the triplet state of the structure shown in Figure 3d. The 2.13 eV binding energy peak measured in the $Nb_2C_5^-$ photodetachment spectra is energetically very similar to the 2.25 eV peak measured for $Nb_2C_4^-$ electron detachment, which was assigned to the two-dimensional planar structure shown in Figure 3b. The computational prediction that best matches the 2.13 eV experimental measurement for $Nb_2C_5^-$ corresponds to the isomer in Figure 3e, which is also a planar two-dimensional structure. The strong similarity between the experimental binding energies and computational results for the $Nb_2C_4^-$ and $Nb_2C_5^-$ structures supports assignment of the 2.25 and 2.13 eV transitions to the isomers shown in Figure 3, panels b and e, respectively. Central to the two- and three-dimensional structures calculated for $Nb_2C_4^-$ and $Nb_2C_5^-$ is Nb−Nb bonding.

Both photodetachment peaks measured for the $Nb_2C_6^-$ cluster (2.01 and 3.06 eV binding energies) are in relative agreement with assignment to the isomer shown in Figure 3h; the peaks with low and high binding energy correspond to the singlet and triplet transitions, respectively. The central moiety of this cluster is a Nb_2C_2 planar ring that closely resembles the structure proposed by Harris and Dance[22] for neutral Nb_2C_2, which could serve as a building block for these clusters. This is the smallest diniobium−carbon cluster size that provides experimental evidence for Nb−C bonding being preferential to Nb−Nb bonding.

The two measured photoelectron peaks of $Nb_2C_7^-$ (2.01 and 3.06 eV binding energies) are in good agreement with computational predications for the lower (septet) and higher transitions of the linear cluster (Figure 3j), with the septet having the lower binding energy. The higher transition is observed as the primary peak. Again, the possible existence of a higher energy isomer present in small abundance is not ruled out. The computational photodetachment values exhibit a strong dependence on the sequence of niobium and carbon atoms in the linear chain. Electron binding energies that best match the experimental photodetachment energies are obtained for structures where the carbon chain is terminated by a single niobium atom at both ends. Attempts to reproduce the experimental values with a linear carbon chain attached to a niobium dimer, as well as isomers with niobium atoms placed in the middle of the chain, failed. The lone photoelectron peak (2.75 eV binding energy) measured for the $Nb_2C_8^-$ cluster does not match predictions for either quintet or septet states of the linear structure. Rather, the geometric structure assigned to the $Nb_2C_8^-$ cluster (Figure 3l) is three-dimensional and contains a central planar Nb_2C_2 moiety, similar to $Nb_2C_6^-$. The low-binding- energy peak measured for $Nb_2C_9^-$ closely matches the prediction for the linear septet state (Figure 3o).

The close match between experiment and theory for each cluster size is shown in Figure 4. The VDEs plotted in Figure 4a correspond to nonlinear geometries, that is, three-dimensional and planar two-dimensional structures. An increase of the number of carbon atoms results in an overall increase in the electron binding energies. The comparisons presented in Figure 4b correspond to lower (septet) and higher photodetachment transitions of linear isomers. Linear structures are observed only for clusters containing an odd number of atoms; concomitant increases in electron binding energy and cluster size are observed. These finding are consistent with previous observation on pure linear carbon clusters.[24,25]

To discuss our experimental measurements in light of niobium substitution for carbon, it is first necessary to

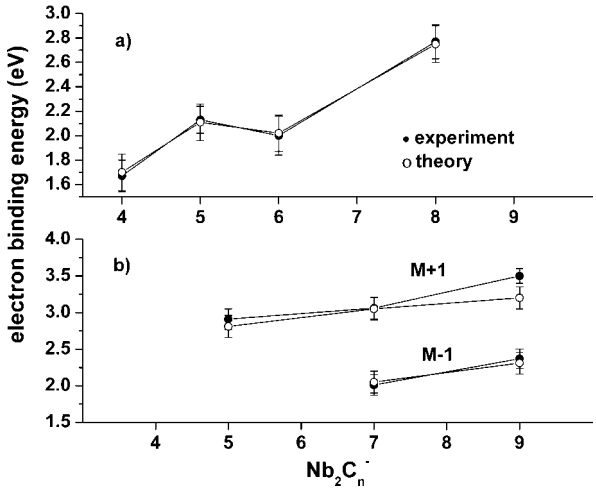

Figure 4. Comparison of experimental and computational electron binding energies (eV) of $Nb_2C_n^-$ ($4 \leq n \leq 9$) clusters. Experimental values are obtained from the spectra shown in Figure 2 with fixed photodetachment energies. The results in panel a compare vertical detachment energies of nonlinear isomers to computational predictions. Energies of M + 1 and M − 1 transitions of linear isomers are compared in panel b. All experimental values are reported to 2σ deviation.

review existing literature on pure carbon and mono-metal–carbon clusters. Low- and high-binding-energy features have been observed previously in the anion photodetachment spectra of both pure carbon clusters[24,25] and mono transition metal–carbon-rich clusters.[26–30] These have been assigned to electron detachment from the ground state of two different isomers. The low-energy feature observed in pure carbon clusters is attributed to monocyclic rings.[24] These prior studies report an odd–even alternation of the vertical electron affinity, where clusters containing an even number of carbon atoms exhibit lower electron affinities than those containing an odd number of carbon atoms. The low electron affinity arises from a shell closing for monocyclic rings with an even number of carbon atoms, which results in an enhanced stability for the neutral ground state when compared to those containing an odd number of carbons. Conversely, shell closings occur for the linear isomer when the cluster contains an odd number of carbons, resulting in a $^1\Sigma^+$ ground state as opposed to the open-shell $^3\Sigma^-$ ground state that results from even-membered chains.[31] Experimentally, this is reflected as an even–odd alternation, where clusters comprising an odd number of atoms exhibit the lowest electron affinity, consistent with theoretical calulations.[31] Linear isomers with an odd number of total atoms are found to be especially stable.[25] The low- and high-binding-energy features are documented in anion photodetachment spectra by Wang and co-workers[26] in mononiobium carbides and is attributed to the transition from the anionic ground state to the neutral ground state of the monocyclic ring and linear isomers, respectively. The electron affinities assigned here to the linear Nb_2C_n isomers track very well with those observed for the pure carbon and mononiobium–carbon clusters but with slightly lower electron affinity. This is likely owing to the presence of niobium, which has a much lower electron affinity (0.893 eV)[32] than all carbon clusters considered in this manuscript. This also suggests the linear anion-to-linear neutral transition is centered on the niobium atom. All VDEs measured previously for linear mononiobium carbon clusters fall within the range of 2.5–4.0 eV, in relative agreement with those reported here, which for the diniobium–carbon system ranged from 2.0 to 3.6 eV.

Our data indicate that the dominant isomer for the Nb_2C_7 cluster is one with a linear structure. In addition, independently conducted theoretical and experimental studies have concluded that the C_9 species of the pure carbon analogue is most stable in linear form.[24,25,33] Linear isomers of Nb_2C_5 and Nb_2C_9 are also observed here. With regard to our present data, this is consistent with the notion that niobium can replace an atom in a carbon network with the Nb_2C_7 taking on some of the character of C_9 and, likewise, Nb_2C_5 and Nb_2C_9 for C_7 and C_{11}, respectively.

Upon formation of the Nb_2C_8 cluster, a single feature with a measured VDE of 2.75 eV was observed in the electron kinetic energy spectrum, corresponding to a nonlinear structure. The results from Arnold *et al.*[25] confirm assignment of linear anionic clusters for C_2–C_9 and C_{11}; however, no evidence for linear C_{10}^- is found. In keeping with the analogy of niobium substitution for carbon, the analogue to C_{10} for the diniobium series is Nb_2C_8, which also shows no evidence for a linear isomer. The VDE of Nb_2C_9 was determined to be 2.37 eV, assigned to the linear isomer in the septet electronic state; the spectrum also contains a higher energy feature at 3.57 eV, which may correspond to the higher linear state energy. This assignment agrees well with the experimental data of Smalley and co-workers[24] on pure carbon anions, in which a linear geometric structure in the singlet electronic state was found for the C_{11}^- species. The enhanced stability that we report here for linear diniobium–carbon clusters containing an odd number of atoms, and the lack of a linear Nb_2C_8 species, directly replicates the behavior of pure carbon clusters.

To summarize, the photoelectron spectra indicate that carbon-rich diniobium–carbon clusters exist in multiple isomeric forms. The low-binding-energy peak measured in the $Nb_2C_4^-$ photodetachment spectrum is assigned to the singlet state of the three-dimensional structure shown in Figure 3a. This structure is similar to that measured for the V_2C_4 anion[23] and consists of two NbC_2 moieties believed to be important for the formation of larger metal carbides. The peak measured at 2.25 eV binding energy is assigned to the planar isomer

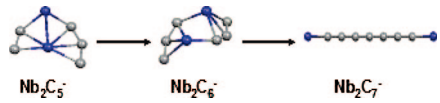

Figure 5. Schematic representation of bonding arrangements of $Nb_2C_n^-$ ($5 \leq n \leq 7$) clusters using computationally determined structures. The illustration depicts the significant influence of cluster size; addition of only a single carbon atom dramatically alters the formed cluster geometry.

in Figure 3b. The calculated structure of $Nb_2C_5^-$, shown in Figure 3e, matches the binding energy of the experimentally measured 2.13 eV peak. The planar geometry of the $Nb_2C_5^-$ cluster is very similar to the $Nb_2C_4^-$ isomer corresponding to the 2.25 eV photodetachment peak. For both species, the cluster is formed by a Nb−Nb dimer that is bridged by C_2 and C_3 units. A similar growth pattern was predicted over a broad cluster range by Harris and Dance.[22]

The $Nb_2C_6^-$ cluster forms primarily through Nb−C bonding, with no direct Nb−Nb bonds. In going to $Nb_2C_7^-$, only photoelectron peaks corresponding to a linear structure are observed. Linear isomers are also observed for $Nb_2C_5^-$ and $Nb_2C_9^-$. For all sizes considered here, a carbon chain is terminated by a single niobium atom at each end. The photodetachment spectrum of $Nb_2C_8^-$ contains a single peak at 2.75 eV binding energy, assigned to the structure in Figure 3l. A transition from Nb−Nb-centered bonding to niobium-separated moieties is observed. This finding is consistent with previous work[22] that showed Nb−C bonding is preferentially stabilizing, followed by C−C bonding, while Nb−Nb bonding is much less significant. Interestingly, the $Nb_2C_6^-$ and $Nb_2C_8^-$ isomers, shown in Figure 3, panels h and l, include a central Nb_2C_2 moiety that matches the planar Nb_2C_2 ring structure calculated previously,[22] but with multiple bridging NbC_2 units that bend out-of-plane. The nonlinear geometries likely deviate slightly from planar structures due to increased ring strain in the binary system.

The experimental photoelectron measurements, compared with computational results, clearly show the diniobium−carbon clusters exist in several structural motifs. Moreover, abrupt changes are observed over a small, critical size range. Incorporation of only a single additional carbon atom, in going from $Nb_2C_5^-$ to $Nb_2C_6^-$ and again to $Nb_2C_7^-$, induces a dramatic alteration in the dominant geometric isomer. This trend is shown schematically, with computational structures, in Figure 5. These findings support suggestions that the niobium−carbon system is a versatile one for the development of CAMs. It is also clear that formation of desired "target" species is likely highly dependent on nucleation conditions.

It has been suggested previously[9] that niobium may readily substitute carbon in large networks. To our knowledge, the present study, that investigates both electronic and geometric structures of $Nb_2C_n^-$ clusters, provides the most direct evidence of this behavior. Our own research has shown that vanadium carbides in this size range, generated under similar source conditions, are likely formed by an ionic interaction between the metal and carbon.[23] Other groups have reported analogous results for early transition metals.[34] Niobium, on the other hand, may form a covalent linkage with carbon;[22] this is likely the reason it substitutes readily for carbon. Niobium is unique because it is the first Group V metal to display an s-to-d electron promotion, resulting in four d valence electrons and an open s orbital. This electron promotion is likely responsible for the unique bonding behavior exhibited by niobium−carbon clusters. The four d electrons may hybridize and form covalent bonds similar to those formed by sp-hybridized carbon, and the open s orbital is available for strong σ bonding between the metal and carbon. Conversely, earlier transition metals such as titanium and vanadium do not promote an s electron; they have only two and three d valence electrons, respectively, and the s orbitals are filled. This results in preferential ionic bonding between the metal and carbon. We have demonstrated that niobium mediates growth of a diverse and complicated array of clusters, whereas vanadium restricts it when source conditions favor high-carbon-content clusters.[23] This finding likely arises from the difference between the covalent and ionic bonds made with carbon by niobium and vanadium, respectively. As stated above, our cluster source temperatures are likely high; therefore, linear chains may be more dominant. Many pure carbon clusters of cyclic geometry obey Hückel's rule and may exhibit aromaticity (for example, $n = 6$ and 10).[33] Niobium replacement of carbon provides an opportunity to explore metal-containing aromatic molecules, which we are actively pursuing. Also, the possible incorporation of other metals such as chromium ($3d^54s^1$) and tungsten ($5d^46s^2$) in the carbon network is under study. Studies of these metals will provide significant insight into the influence of the promotion of the valence electron from the s to the d orbital on the metal–carbon interaction.

In conclusion, we have investigated the evolving electronic and geometric properties of carbon-rich diniobium−carbon clusters as a function of cluster size. We present clear evidence for the coexistence of multiple isomers and find a strong size dependence on the preferred geometry. The linear isomer is observed for clusters containing an odd number of atoms, which is commonly seen for pure carbon clusters. In fact, the spectra agree well with those obtained for analogous carbon clusters, in support of niobium substitution for carbon in a network. The data suggest that, for cluster sizes between Nb_2C_7 and Nb_2C_9, the behavior directly mimics that of pure carbon, including the absence of linear Nb_2C_8. A detailed study of the organometallic

chemistry of niobium−carbon systems would seem to be a very promising endeavor for new discoveries.

METHODS

Experimental Procedures for Cluster Formation and Anion Photoelectron Spectroscopy. A detailed description of the experimental apparatus is the primary focus of a separate report,[11] and as such only a brief overview will be provided here. Niobium−carbon clusters are generated in a 10 Hz laser vaporization plasma reactor source in which the second harmonic (532 nm, 1 mJ/pulse) of a Nd:YAG laser is focused on a translating and rotating niobium rod, forming a plasma. Typically, a helium carrier gas is seeded with 10% methane and passed over the plasma, leading to the dehydrogenation of methane and the formation of metal–carbon clusters. The anions are subsequently pulse extracted, and the cluster distribution is analyzed by a linear time-of-flight mass spectrometer. The resolution ($m/\Delta m$) of the mass spectrometer is currently greater than 500, which is more than sufficient for the cluster sizes studied here. The cluster of interest is then mass selected prior to photodetachment. Following mass selection, electrons are detached with a XeCl excimer laser (308 nm, 3.02 eV). Detached electrons are collected by a "magnetic bottle" type photoelectron spectrometer, where a strong (1 T) permanent magnet is used to collect electrons over 4π radians. The detached electrons traverse a low-field (10^{-3} T) drift region before detection by a Z-stack microchannel plate (MCP) detector. The measured ion current from the MCP is then amplified before collection by a digital oscilloscope and is transferred to a PC for analysis. The magnetic bottle electron kinetic energy analyzer is calibrated daily by photodetachment of Cu^-. The known photodetachment spectrum[32] of Cu^- includes transition from the Cu^- ground state ($^1S_0$, $3d^{10}4s^2$) to the Cu ground state ($^2S_{1/2}$, $3d^{10}4s^1$) as well as the first two Cu excited states ($^2S_{5/2}$, $3d^94s^2$; ($^2S_{3/2}$, $3d^94s^2$). The electron kinetic energy resolution of the experiments is better than 150 meV at 1.2 eV.

Computational Procedures. First-principle electronic structure investigations on Nb_2C_n clusters were carried out in a GGA within the density functional formalism.[12] Full geometry optimizations were performed using the deMon2k software.[13] In order to avoid the calculation of four-center electron repulsion integrals, the variational fitting of the Coulomb potential[14,15] was employed. The numerical integration of the exchange-correlation energy and potential was performed on an adaptive grid.[16] The exchange and correlation effects were incorporated using the functional proposed by Perdew, Burke, and Ernzerhof.[17] A DZVP basis set[18] was used for the carbon atoms, and the Nb atom was described using the 13-electron scalar QECP proposed by Andrae *et al.*[19] in combination with the LANL2DZ[20] valence basis. The auxiliary density was expanded in primitive Hermite Gaussian functions using the A2 auxiliary function set for C atoms and the GEN-A2* auxiliary function set for Nb. A half-numeric integrator was employed for the ECP integrals.[21]

Acknowledgment. The authors gratefully acknowledge support by the U.S. Air Force Office of Scientific Research, Grant FA9550-04-1-0066. S.N.K. and J.U.R. acknowledge support from the U.S. Air Force Office of Scientific Reasearch Grant. FA9550-05-1-0186. P.A.C. acknowledges support from the Department of the Army through MURI grant no. W911NF-06-1-0280.

REFERENCES AND NOTES

1. Guo, B. C.; Kerns, K. P.; Castleman, A. W., Jr. $Ti_8C_{12}^+$ Metallocarbohedrenes−A New Class of Molecular Clusters. *Science* **1992**, *255*, 1411–1413.
2. Sakurai, H.; Castleman, A. W., Jr. Ionization Potentials for the Titanium, Zirconium, and the Mixed Metal Met-Cars. *J. Phys. Chem. A* **1998**, *102*, 10486–10492.
3. Stairs, J. R.; Davis, K. M.; Peppernick, S. J.; Castleman, A. W., Jr. Delayed Ionization of the Zirconium Met-Car, Zr_8C_{12}. *J. Chem. Phys.* **2003**, *119*, 7857–7863.
4. Leskiw, B. D.; Knappenberger, K. L.; Castleman, A. W., Jr. Relaxation Dynamics of the Electronically Excited Vanadium Met-Car Cluster. *J. Chem. Phys.* **2002**, *117*, 8321–8326.
5. Liu, P.; Rodriguez, A.; Muckerman, J. T. Desulfurization of SO_2 and Thiophene on Surfaces and Nanoparticles of Molybdenum Carbide: Unexpected Ligand and Steric Effects. *J. Phys. Chem. B* **2004**, *108*, 15662–15670.
6. Castleman, A. W., Jr.; Bowen, K. H. Clusters: Structure, Energetics, and Dynamics of Intermediate States of Matter. *J. Phys. Chem.* **1996**, *100*, 12911–12944.
7. Walters, R. S.; Schleyer, P. V.; Corminboeuf, C.; Duncan, M. A. Structural Trends in Transition Metal Cation−Acetylene Complexes Revealed through the C−H Stretching Fundamentals. *J. Am. Chem. Soc.* **2005**, *127*, 1100–1101.
8. Wei, S.; B. C. Guo; Deng, H. T.; Kerns, K.; Purnell, J.; Buzza, S. A.; Castleman, A. W., Jr. Formation of Met-Cars and Face-Centered-Cubic Structures−Thermodynamically or Kinetically Controlled. *J. Am. Chem. Soc.* **1994**, *116*, 4475–4476.
9. Wei, S.; Guo, B. C.; Purnell, J.; Buzza, S.; Castleman, A. W., Jr. Metallo-Carbohedrenes−Formation of Multicage Structures. *Science* **1992**, *256*, 818–820.
10. Shelimov, K. B.; Clemmer, D. E.; Jarrold, M. F. Metal-Containing Carbon Clusters. *J. Chem. Soc., Dalton Trans.* **1996**, 567–574.
11. Knappenberger, K. L, Jr.; Jones, C. E., Jr.; Sobhy, M. A.; Castleman, A. W., Jr. Versitle Cluster-Based Photoelectron Spectrometer. *Rev. Sci. Instrum.* **2006**, *77*, 123901.
12. Kohn, W.; Sham, L. S. Self-Consistent Equations Including Exchange and Correlation Effects. *Phys. Rev.* **1965**, *140*, A1133–A1138.
13. Köster, A. M.; Calaminici, P.; Casida, M. E.; Flores-Moreno, R.; Geudtner, G.; Goursot, A.; Heine, T.; Ipatov, A.; Janetzko, F.; del Campo, J. M.; *et al. deMon2k*, v. 2.3; deMon Developers, 2006.
14. Dunlap, B. I.; Connolly, J. W. D.; Sabin, J. R. On First-Row Diatomic Molecules and Local Density Models. *J. Chem. Phys.* **1979**, *71*, 4993–4999.
15. Mintmire, J. W.; Dunlap, B. I. Fitting the Coulomb Potential Variationally in Linear-Combination-of-Atomic-Orbitals Density-Functional Calculations. *Phys. Rev. A* **1982**, *25*, 88–95.
16. Köster, A. M.; Flores-Moreno, R.; Reveles, J. U. Efficient and Reliable Numerical Integration of Exchange-Correlation Energies and Potentials. *J. Chem. Phys.* **2004**, *121*, 681–690.
17. Perdew, J. P.; Burke, K.; Ernzerhof, M. Generalized Gradient Approximation made simple. *Phys. Rev. Lett.* **1996**, *77*, 3865–3868.
18. Godbout, N.; Salahub, D. R.; Andzelm, J.; Wimmer, E. Optimization of Guassian-type Basis-Sets for Local Spin-Density Functional Calculations. 1. Boron through Neon, Optimization Technique and Validation. *Can. J. Chem.* **1992**, *70*, 560–571.
19. Andrae, D.; Haeussermann, U.; Dolg, M.; Stoll, H.; Preuss, H. Energy-adjusted Ab Initio Pseudopotentials for the Second and Third Row Transition-Elements. *Theor. Chim. Acta* **1990**, *77*, 123–141.
20. Hay, P. J.; Wadt, W. R. *Ab initio* Effective Core Potentials for Molecular Calculations. Potentials for the Transition-Metal Atoms Sc to Hg. *J. Chem. Phys.* **1985**, *82*, 270–283.
21. Flores-Moreno, R.; Alvarez-Mendez, R. J.; Vela, A.; Köster, A. M. Half-Numerical Evaluation of Pseudopotential Integrals. *J. Comput. Chem.* **2006**, *27*, 1009–1019.
22. Harris, H.; Dance, I. The Geometric and Electronic Structures of Niobium Carbon Clusters. *J. Phys. Chem. A* **2001**, *105*, 3340–3358.
23. Knappenberger, K. L, Jr.; Jones, C. E., Jr.; Sobhy, M. A.; Iordanov, I.; Sofo, J.; Castleman, A. W., Jr. Anion Photoelectron Spectroscopy and Density Functional Investigation of Vanadium Carbide. *J. Phys. Chem. A* **2006**, *108*, 12814–12821.

24. Yang, S.; Taylor, K. J.; Craycraft, M. J.; Conceicao, J.; Pettiette, C. L.; Chesnovsky, O.; Smalley, R. E. UPS of 2–30-Atom Carbon Clusters: Chains and Rings. *Chem. Phys. Lett.* **1988**, *144*, 431–436.
25. Arnold, D. W.; Bradforth, S. E.; Kitsopoulos, T. N.; Neumark, D. M. Vibrationally-Resolved Spectra of C2-C11 by Anion Photoelectron-Spectroscopy. *J. Chem. Phys.* **1991**, *95*, 8753–8764.
26. Fan, J. W.; Lou, L.; Wang, L. S. FeC_n^- and FeC_nH^- (n=3,4): A Photoelectron Spectroscopic and Density-Functional Study. *J. Chem. Phys.* **1995**, *102*, 2701.
27. Zhai, H.; Liu, S. R.; Li, X.; Wang, L. S. Photoelectron Spectroscopy of Mono-Niobium Carbide Clusters NbC_n^- (n=2–7): Evidence for a Cyclic to Linear Transition. *J. Chem. Phys.* **2001**, *115*, 5170–5178.
28. Wang, X. B.; Ding, C. F.; Wang, L. S. Vibrationally-Resolved Spectra of TiC_x^- (x = 2–5) Clusters. *J. Phys. Chem. A* **1997**, *101*, 7699–7701.
29. Suzuki, S.; Kohno, M.; Siromaru, H.; Achiba, Y.; Kietzmann, H.; Kessler, B.; Gantefor, G.; Eberhardt, W. Time-of-Flight Mass and Photoelectron Spectroscopy study of LaC_n^-. *Z. Phys. D* **1997**, *40*, 407–409.
30. Kohno, M.; Suzuki, S.; Siromaru, H.; Kobayashi, K.; Nagase, S.; Achiba, Y.; Kietzmann, H.; Kessler, B.; Gantefor, G.; Eberhardt, W. Photoelectron Spectroscopy study of MC_n^- (M=Sc, Y, and La, $5 <= n <= 20$). *J. Electron Spectrosc.* **2000**, *112*, 163–173.
31. Ewing, D. W.; Pfeiffer, G. V. Strucutres and Properties of Linear C_n Molecules. *Chem. Phys. Lett.* **1982**, *86*, 365–368.
32. Hotop, H.; Lineberger, W. C. Binding-Energies in Atomic Negative-Ions. 2. *J. Phys. Chem. Ref. Data* **1985**, *14*, 731–750.
33. Raghavachari, K.; Binkley, J. S. Structure, Stability, and Fragmentation of Small Carbon Clusters. *J. Chem. Phys.* **1987**, *87*, 2191–2197.
34. Tono, K.; Terasaki, A.; Ohta, T.; Kondow, T. Geometric and Electronic Structures of $V_2C_2^-$ and V_2C_2 Studied by Photoelectron Spectroscopy and Density-Functional Calculations. *Chem. Phys. Lett.* **2002**, *351*, 135–141.